NASA Technical Memorandum 102828

Turbulence Modeling for Sharp-Fin-Induced Shock Wave/Turbulent Boundary-Layer Interactions

C. C. Horstman

October 1990

National Aeronautics and Space Administration

NASA Technical Memorandum 102828

Turbulence Modeling for Sharp-Fin-Induced Shock Wave/Turbulent Boundary-Layer Interactions

C. C. Horstman, Ames Research Center, Moffett Field, California

October 1990

National Aeronautics and
Space Administration

Ames Research Center
Moffett Field, California 94035-1000

Turbulence Modeling for Sharp-Fin-Induced Shock Wave/Turbulent Boundary-Layer Interactions

C. C. HORSTMAN

NASA Ames Research Center
Moffett Field, CA 94035 USA

Abstract

Solutions of the Reynolds-averaged Navier-Stokes equations are presented and compared with a family of experimental results for the three-dimensional interaction of a sharp-fin-induced shock wave with a turbulent boundary layer. Several algebraic and two- equation eddy-viscosity turbulence models are employed. The computed results are compared with experimental surface pressure, skin-friction, and yaw angle data as well as the overall size of the interaction. Although the major features of the flow fields are correctly predicted, several discrepancies are noted. Namely, the maximum skin-friction values are significantly under-predicted for the strongest interaction cases. These and other deficiencies are discussed.

Introduction

Shock wave/turbulent boundary layer interaction constitutes one of the fundamental problems of modern high-speed fluid dynamics. One simple geometry that produces a complex three-dimensional, separated flow field consists of a sharp fin mounted on a flat-plate surface (Fig. 1). This configuration has been investigated experimentally [1-7] and computationally [2-9] for a wide range of test conditions. Computations have been successful in predicting the essential features of these flow fields, as well as helping to provide a model for the flow field structure. However deficiencies in the computed results have been noted. Two notable defects are the inability to predict the upstream extent of the interaction and the experimentally observed secondary separation [1,2,7]. Direct measurements of surface skin friction [7] are now available for a direct test of the turbulence models employed in the computations. This paper presents a series of computational results using various eddy-viscosity turbulence models to investigate these deficiencies and to test these models' ability to predict the new skin-friction results.

Description of Computations

The governing equations used to describe the flow field are the full compressible mean three-dimensional Navier-Stokes equations using mass-averaged variables in strong conservation form. Their restrictions include the calorically-perfect-gas assumption, the Sutherland viscosity law, and zero bulk viscosity. Four eddy-viscosity models are employed for turbulence closure: the algebraic models of Baldwin-Lomax [10] and Cebeci-Smith [11], which are integrated to the wall, and a two-equation eddy-viscosity (k-ε) model with either wall-function boundary conditions [12] or integration-to-the-wall using the Jones-Launder low-Reynolds-number terms [13]. Further details of the boundary conditions and algorithm used are given in Refs. 6 and 8.

The computational domain extends from a prescribed upstream boundary where an equilibrium turbulent boundary layer is generated (matching the experimental data) to a point well downstream of the interaction. For most of the results presented here the grid was generated so as to take advantage of the experimentally observed quasi-conical flow field. In the x-y (horizontal) plane the grid was developed using a family of rays originating from a virtual origin slightly upstream of the fin leading-edge. Ahead of the interaction these rays were replaced by lines of constant y (spanwise direction). In the x- (streamwise) direction, constant spacing was used. In the z- (vertical) direction an exponentially stretched spacing was used, concentrating most of the points within the boundary layer. When integrating to the wall, the maximum value of z+ for the first grid point was 1.0 in the interaction region. The resulting grid spacing in the x- and y-directions was approximately equal to 0.5 δ_0. The total computational domain encompassed $64 \times 64 \times 40$ grid points in the x-, y-, and z-directions, respectively. For a few computations made for the higher fin angles, the grid in the horizontal plane consisted of lines parallel to the fin and lines of constant x. The x and z spacing was identical to the previously described grid with the same total number of points. In the y-direction the grid spacing was approximately equal to δ_0.

Results and Discussion

Solutions using the four turbulence models have been obtained for fin angles of 10 and 16 degrees at Mach 3 and for 16 and 20 degrees at Mach 4. Solutions using a single model (k-ε integrated to the wall) have been obtained for fin angles of 25 and 30 degrees at Mach 4. The upstream boundary conditions were chosen to match the experimental boundary conditions for the Penn State experiments [2,3,7]. This paper will concentrate on the Mach 4 results where the interactions are the strongest.

The computed and experimental values of skin-friction coefficient are compared for Mach 4 at fin angles of 16 and 20 degrees in Figs. 2 and 3, respectively. The results are plotted in terms of the conical angle β (defined in Fig. 1) at a radial distance from the fin apex of 8.9 cm. Error bars indicating the accuracy of the data are also shown on the figures. Only two computed results are shown for each fin angle. Results obtained with the Baldwin- Lomax turbulence model are close to those shown for the Cebeci-Smith model, and for the k-ε model the use of wall functions did not significantly change the integration-to-the-wall skin friction values which are plotted. It is first noted that the location and magnitude of the peak skin friction are not predicted by any turbulence model. For a fin angle of 16 degrees. the peak values of skin friction are underpredicted by 12% using the algebraic model and 40% using the k-ε model. For 20 degrees the peak values are underpredicted by 40% and 52%, respectively. For both fin angles the algebraic models come closer to the experimental data than the k-ε models.

In an attempt to assess the effect of grid resolution, a second calculation was made for the 20-degree case using a coarser grid. The k-ε integration-to-the-wall model was used. The y-spacing of the finer grid is half that of the coarser one, resulting in $\Delta\beta = 0.5$ and 1.0 degree respectively, near the peak skin-friction location. No change in computed maximum skin friction was noted. This may be an indication that the underpredictions are due to inadequate turbulence modeling, rather than to inadequate grid resolution. Of course, the proper way to do grid resolution studies is to halve the grid in all three directions, but this is not presently feasible because of computer limitations.

The computed and experimental values of surface pressure are compared at Mach 4 for a fin angle of 20 degrees in Fig.4. Error bars indicating the accuracy of the data are shown. Little difference is seen between the two turbulence models also shown. The two other models give similar results. The computed results predict the correct spanwise extent and peak value, but do not show the experimentally observed local pressure minimum near $\beta = 30$ degrees. This low pressure occurs because of the high reversed velocity resulting from an image effect, or so-called ground effect, of the vortex which dominates this flow field [8,14]. Based on this result it would seem that the present computations underpredict the strength of the vortex, resulting in lower velocities near the wall, thus underpredicting the surface skin friction and overpredicting the surface pressure under the vortex. Comparisons with the pressure data obtained at a fin angle of 16 degrees give similar results.

Although not shown here, comparisons have also been made between the experimental and computed surface pressure and skin- friction results for fin angles of 10 and 16 degrees at Mach 3. A few comparisons are shown in Ref. 3. In general the agreement between theory and experiment is better for Mach 3 than the Mach 4 results shown here. This can be best shown

by plotting the peak skin-friction values vs. the pressure ratio across the undisturbed inviscid fin shock wave, as shown in Fig. 5. The first two experimental points are for Mach 3, $\alpha = 10$ and 16 degrees, and the second two for Mach 4, $\alpha = 16$ and 20 degrees. It can clearly be seen that the measured peak skin-friction values rise in a monotonic but nonlinear fashion with increasing shock strength. In contrast, the k-ε prediction increases almost linearly with interaction strength and becomes progressively inaccurate as the interaction strength is increased. The prediction using the Cebeci-Smith model shows better agreement for weak- and moderate-strength interactions, but falls off dramatically for the stronger interactions.

Figure 6 shows comparisons of the angles of the surface skin- friction lines, ϕ, plotted against β for = 16 degrees, Mach 4. Three calculations are shown. Results obtained with the Baldwin-Lomax model do not differ from those shown for the Cebeci-Smith model. The calculated results using the Cebeci-Smith and k-ε integrated-to-the-wall (ITW) models show reasonable agreement with the data. However, the k-ε wall function (WF) model solution grossly underpredicts the angular extent of the measured upstream influence. These results show that integration to the wall appears to have solved the nagging problem of underprediction of the upstream influence of such interactions in several previous publications [2,6-9] where k-ε wall-function turbulence modeling was used. For the Mach 4, $\alpha = 20$ degree case, the results and conclusions are similar to those discussed here.

It was shown above that the predicted upstream influence changes significantly depending on the use of wall functions or integration- to-the-wall. This is due to the implicit assumption, in the wall- function case, that there is no flow turning below the second grid point away from the wall. Two examples of computed flow yaw-angle profiles shown in Fig. 7 illustrate this point (yaw angle is defined as the direction of the velocity vector in the x-y plane). In this figure the computed yaw angle at each grid point is plotted vs. z and z+ for the Mach 4, $\alpha = 16$ degree interaction. The locations of these profiles are $\beta = 40$ degrees (wall functions) and $\beta = 43$ degrees (integration to the wall), both near the upstream-influence line of the interaction. It is seen that the predicted yaw angle increases significantly in the region very close to the wall, well below the minimum-height grid point employed by the wall-function treatment. This increases the upstream influence and eventually affects the entire flow field. Thus, any future wall-function computations for this class of swept interactions should definitely allow for additional turning below the first two grid points. (Work is in progress to accomplish this.)

Experimental and computed values of the extent of upstream influence are compared for Mach 4 in Fig.8. Here we are plotting the angle of the separation line, β_s, vs. the fin angle, α. β_s was obtained from the measured or calculated surface-shear line patterns far downstream

from the fin leading edge. (See Fig. 9 for a computed example). Two experimental data sets are shown, one obtained by Zheltovodov et al. [1] and the other by Settles and his co-workers [2,7]. The two data sets are in remarkable agreement. Computed results are also shown using two turbulence models; k-ε integrated to the wall and k-ε wall functions. The integrated-to-the-wall results are in much better agreement with the data than the wall-function results. For $\alpha < 20$ degrees these computations are certainly within the experimental uncertainties of these measurements. However, for $\alpha > 20$ degrees the computations and experimental results diverge, with the computations underpredicting β_s by 15% at $\alpha = 30$ degrees. Results obtained with the two algebraic turbulence models give values of β_s similar to those obtained for the k-ε integrated-to-the-wall computations. At 20 degrees, computed values of β_s for both the coarse and fine grids were almost identical. The reasons for the discrepancy at large fin angles are not known. Work is in progress to resolve this issue.

Secondary separation has been observed for these flow fields by most experimenters [1-7]. The experimental evidence of secondary separation comes mostly from an observed feature in the surface skin-friction line patterns. Zheltovodov [1] found two types of secondary separation. For small fin angles a secondary separation line appears near primary separation, and as the fin angle is increased this feature disappears and a second secondary separation is seen near the fin. For Mach 4 the first secondary separation appears at $\alpha = 8$ degrees and vanishes at $\alpha = 19$ degrees, and the second secondary separation is first seen at $\alpha = 23$ degrees.

In a previous publication [9], we reported to have calculated a secondary flow separation for these flow fields for Mach 4 at fin angles of 16 and 20 degrees. However, it has been pointed out by Zheltovodov [15] that the sense of rotation of the computed secondary separation is not consistent with experimental results. Those calculations were made with a k-ε wall-function turbulence model. Since then we have obtained the solutions using both algebraic and k-ε models integrating to the wall. These results did not show any evidence of secondary separation. It is now felt that the previously computed secondary separation is purely an artifact of the turbulence model used and does not reflect the true physics of the flow field.

The current work extended the computations to fin angles up to 30 degrees in search of the second appearance of secondary separation. The computed surface-shear-line pattern for Mach 4, $\alpha = 30$ degrees is shown on Fig. 9. The k-ε integrated-to-the-wall turbulence model was used. No evidence of secondary separation is observed; only the large primary separation zone is seen. To further examine this computed flow field, let us look at particle paths confined to a two-dimensional plane normal to the free stream flow direction with the crossflow velocities calculated in approximate conical coordinates. (See Ref. 8 for details.) These special trajectories are shown for the Mach 4, $\alpha = 30$ degree case in Fig. 10. The large primary

vortex is clearly seen, but there is no evidence of secondary separation. In a recent publication [16], Hung has speculated that the secondary oil-accumulation line observed in the experiments is simply a demarcation between regions of high and low surface skin friction and not secondary separation. Further work in grid refinement and nonisotropic turbulence modeling is planned.

Concluding Remarks

Solutions have been obtained for a series of three-dimensional, shock-wave turbulent-boundary-layer interaction flow fields using several turbulence models. As the shock strength increased the peak values of measured skin-friction were underpredicted by as much as 52%. No single turbulence model correctly predicted all the test cases. The simpler algebraic models outperformed the more complex two-equation eddy-viscosity models. When integrating to the wall, all the turbulence models accurately predicted the extent of the interaction for fin angles less than 20 degrees. The use of wall functions (as currently formulated) caused significant underpredictions of the interaction size. For fin angles greater than 20 degrees the interaction size was underpredicted by all the models used. Although secondary separation has been "found" by all the experiments, detailed examination of the computed results indicated no evidence of this additional feature of the flow field.

Although the major features of these flow fields have been successfully computed, there are several deficiencies that have been noted. The reasons for these deficiencies are not known at present. Work on turbulence modeling, grid refinement, boundary conditions, etc. is continuing. Also, heat transfer measurements are planned for these flow fields. This should help the turbulence modeling efforts significantly.

References

1. Zheltovodov, A. A., Maksimov, A. I. and Shilien, E. K., "Development of Turbulent Separated Flows in the Vicinity of Swept Shock Waves," The Interactions of Complex 3-D Flows, edited by Kharitonov, A.M., Akademia Nauk USSR, Inst. Theor. and Appl. Mechanics, Novosibirsk, 1987, pp. 67-91.
2. Lu, F. K., Settles, G. S. and Horstman, C. C., "Mach Number Effects on Conical Surface Features of Swept Shock-Wave/Boundary-Layer Interactions," AIAA Journal, Vol. 28, Jan. 1990, pp. 91-97.
3. Kim, K-S, and Settles, G. S., "Skin Friction Measurements by Laser Interferometry in Swept Shock/Boundary-Layer Interactions," AIAA Journal, Vol. 28, Jan. 1990, pp. 133-139.

4. Settles, G. S. and Dolling, D. S., "Swept Shock Wave/Boundary-Layer Interactions," in Tactical Missile Aerodynamics, AIAA Progress in Astronautics and Aerodynamics Series, Vol. 104, 1986, pp. 297-379.
5. Settles, G. S. and Dolling, D. S., "Swept Shock/Boundary-Layer Interactions—Tutorial and Update," AIAA Paper 90-0375, 1990.
6. Knight, D. D., Horstman, C. C., Shapey, B. and Bogdonoff, S. M., "The Flowfield Structure of the 3-D Shock Wave-Boundary Layer Interaction Generated by a Sharp Fin at Mach 3," AIAA Journal, Vol. 25, Oct. 1987, pp. 1331-1337.
7. Kim, K-S, Lee, Y., Alvi, F. S., Settles, G. S. and Horstman, C. C., "Laser Skin Friction Measurements and CFD Comparison of Weak- to-Strong Swept Shock/Boundary-Layer Interactions," AIAA Paper 90-0378, 1990.
8. Horstman, C. C., "Computation of Sharp-Fin-Induced Shock Wave/ Turbulent Boundary Layer Interactions," AIAA Journal, Vol.24, Sept. 1986, pp. 1433-1440.
9. Horstman, C. C., "Prediction of Secondary Separation in Shock Wave Boundary-Layer Interactions," Computers & Fluids, Vol. 17, Apr. 1989, pp. 611-614.
10. Baldwin, B. S. and Lomax, H., "Thin Layer Approximation and Algebraic Model for Separated Turbulent Flows," AIAA Paper 78-0257, 1978.
11. Cebeci, T. and Smith, A. M. O., Analysis of Turbulent Boundary Layers, Academic Press, New York, 1974.
12. Viegas, J. R., Rubesin, M. W. and Horstman, C. C., "On the Use of Wall Functions as Boundary Conditions for Two-Dimensional Separated Compressible Flows," AIAA Paper 85-0180, 1985.
13. Jones, W. P. and Launder, B. E., "The Prediction of Laminarization with a Two-Equation Model of Turbulence," International Journal of Heat and Mass Transfer, Vol. 15, Feb. 1972, pp. 301-314.
14. Hung, C. M. and Buning, P. G., "Simulation of Blunt-Fin-Induced Shock-Wave and Turbulent Boundary-Layer Interaction," Journal of Fluid Mechanics, Vol. 154, 1985, pp. 163-185.
15. Zheltovodov, A. A., private communication.
16. Hung, C. M., "Computation of Navier-Stokes Equations for Three- Dimensional Flow Separation," NASA TM-102266, Dec. 1989.

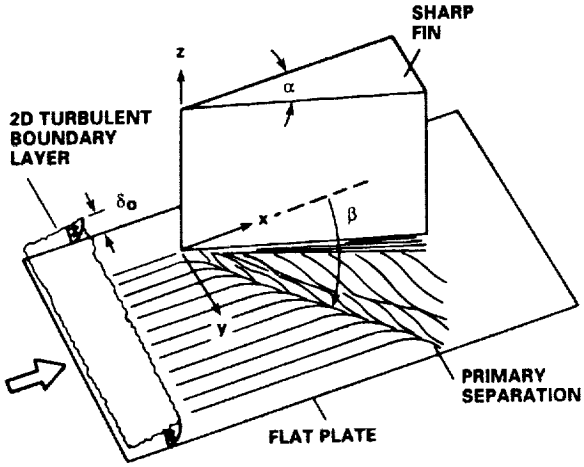

Fig. 1. Flow geometry.

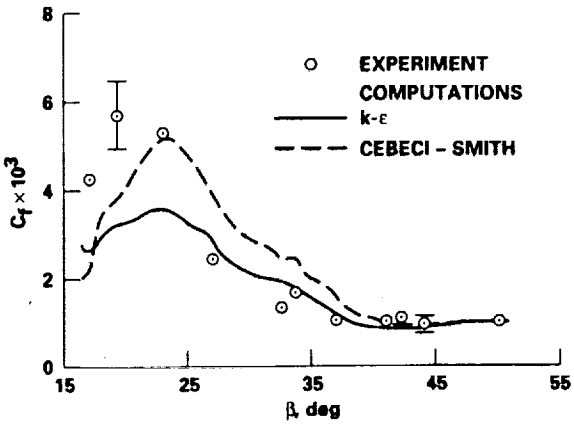

Fig. 2. Comparison of surface skin friction distributions, $\alpha = 16°$, $M_\infty = 4$.

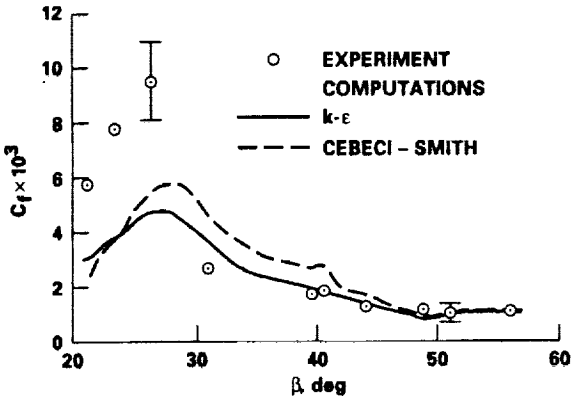

Fig. 3. Comparison of surface skin friction distributions, $\alpha = 20°$, $M_\infty = 4$.

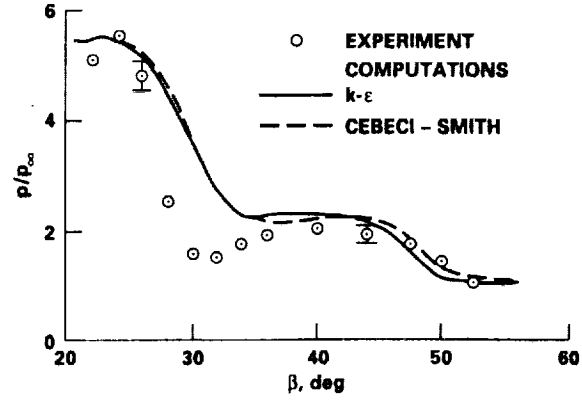

Fig. 4. Comparison of surface pressure distributions, $\alpha = 20°$, $M_\infty = 4$.

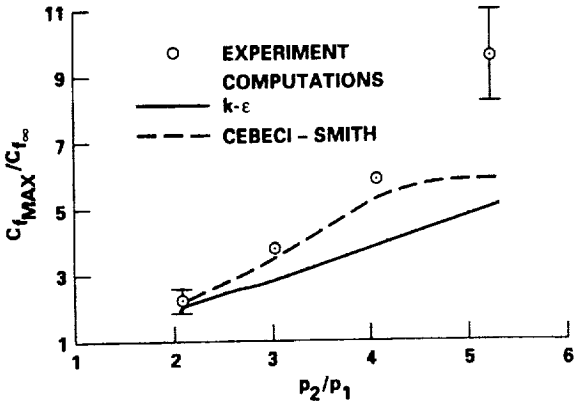

Fig. 5. Comparison of peak skin friction vs. inviscid shock strength.

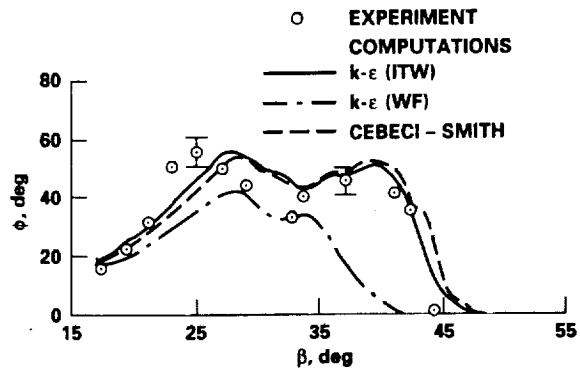

Fig. 6. Comparison of surface skin friction angles, $\alpha = 16°$, $M_\infty = 4$.

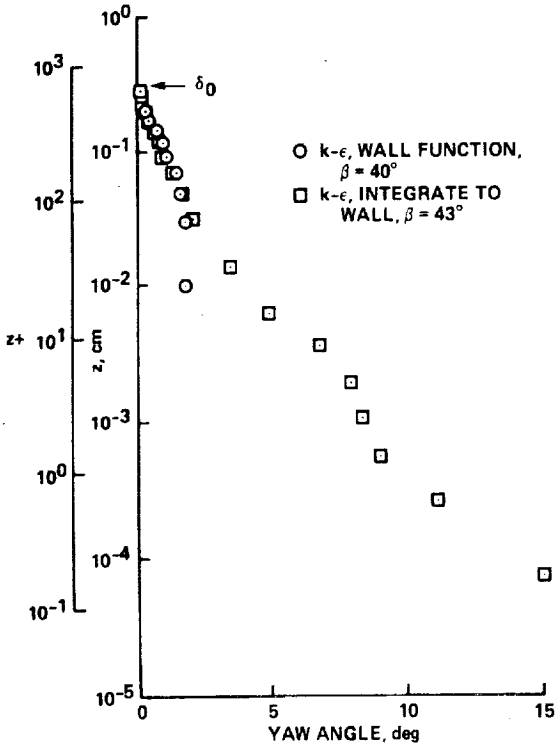

Fig. 7. Yaw angle computations, $\alpha = 16°$, $M_\infty = 4$.

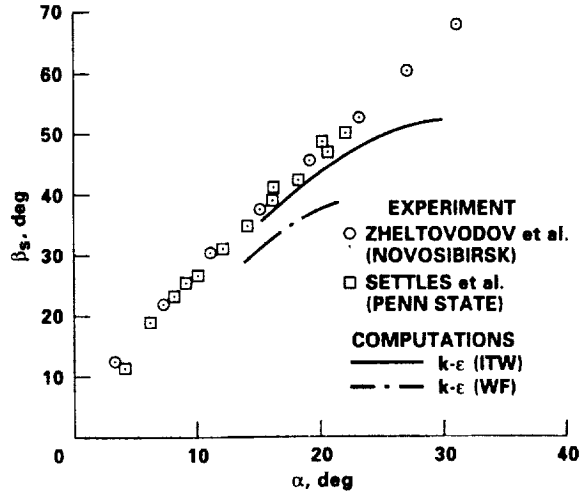

Fig. 8. Comparison of surface separation line angles, $M_\infty = 4$.

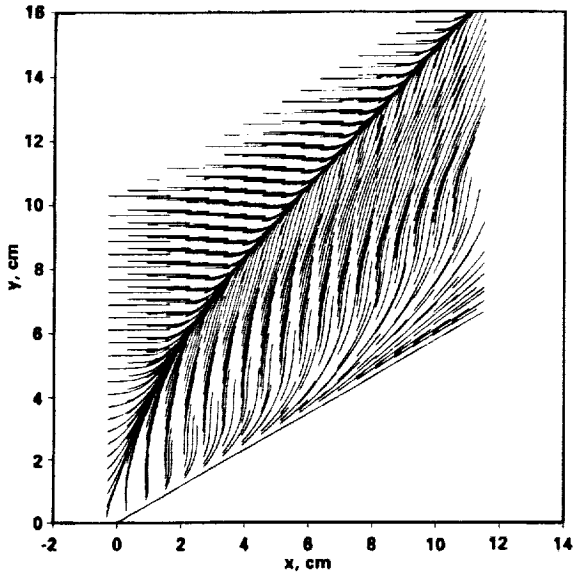

Fig. 9. Computed surface shear lines, $\alpha = 30°$, $M_\infty = 4$.

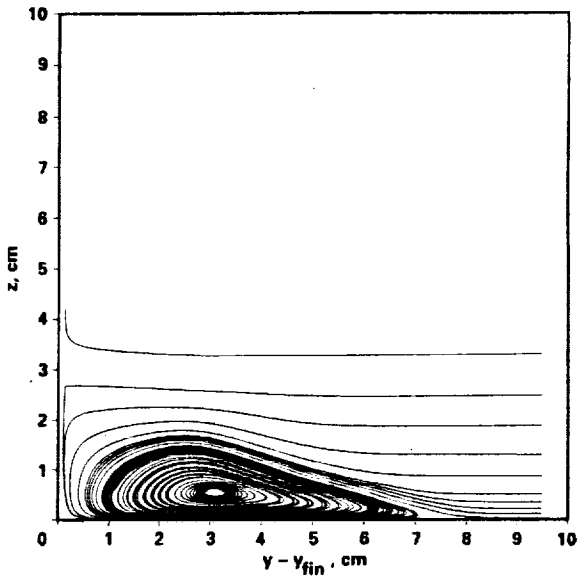

Fig. 10. Computed crossflow velocity trajectories, $\alpha = 30°$, $M_\infty = 4$, x = 8.3 cm.

NASA
National Aeronautics and Space Administration

Report Documentation Page

1. Report No.	2. Government Accession No.	3. Recipient's Catalog No.
NASA TM-102828		

4. Title and Subtitle	5. Report Date
Turbulence Modeling for Sharp-Fin-Induced Shock Wave/ Turbulent Boundary-Layer Interactions	October 1990
	6. Performing Organization Code
7. Author(s)	8. Performing Organization Report No.
C. C. Horstman	A-90172
	10. Work Unit No.
	505-60-11
9. Performing Organization Name and Address	11. Contract or Grant No.
Ames Research Center Moffett Field, CA 94035-1000	
	13. Type of Report and Period Covered
12. Sponsoring Agency Name and Address	Technical Memorandum
National Aeronautics and Space Administration Washington, DC 20546-0001	14. Sponsoring Agency Code

15. Supplementary Notes

Presented at the IUTAM Symposium on Separated Flows and Jets, Novosibirsk, USSR, July 9-13, 1990.

Point of Contact: C. C. Horstman, Ames Research Center, MS 229-1, Moffett Field, CA 94035-1000
(415) 604-6255 or FTS 464-6255

16. Abstract

Solutions of the Reynolds-averaged Navier-Stokes equations are presented and compared with a family of experimental results for the ~~three-dimensional~~ 3-D interaction of a sharp-fin-induced shock wave with a turbulent boundary layer. Several algebraic and two-equation eddy-viscosity turbulence models are employed. The computed results are compared with experimental surface pressure, skin-friction, and yaw angle data as well as the overall size of the interaction. Although the major features of the flow fields are correctly predicted, several discrepancies are noted. Namely, the maximum skin-friction values are significantly underpredicted for the strongest interaction cases. These and other deficiencies are discussed.

17. Key Words (Suggested by Author(s))	18. Distribution Statement
Skin friction CFD Turbulence models	Unclassified-Unlimited Subject Category - 34

19. Security Classif. (of this report)	20. Security Classif. (of this page)	21. No. of Pages	22. Price
Unclassified	Unclassified	13	A02